

Combustion Characteristics of Transverse Hydrogen Jet in a Supersonic Compact Inlet/Combustor Model

Zhi-wei Huang, Guo-Qiang He, Fei Qin, Xiang-geng Wei, Shuai Wang
Science and Technology on Combustion, Internal Flow and Thermal-Structure Laboratory,
Northwestern Polytechnical University
Xi'an, Shaanxi, PR. China

1 Abstract

This paper studies combustion characteristics of hydrogen in a compact supersonic inlet/combustor model numerically. Three-dimensional compressible large eddy simulation (LES) based on an Open Source Field Operation and Manipulation (OpenFOAM) solver is performed on a hydrogen-fueled combustor under the nominal inflow conditions of flight Mach number at 8.0. The partially stirred reactor (PaSR) combustion model is adopted to account for the sub-grid turbulence-chemistry interactions. A skeletal mechanism for hydrogen combustion kinetics including 9 species, 27 reaction steps is used to depict the ensuing flow and combustion process on structured hexahedral grids. Special attentions are paid on the inlet-induced shock / the injector-induced shock, the injector-induced shock / the central reacting layer, and the injector-induced shock / flame interactions. The combustion efficiency is calculated. The combustion process in the model configuration is intrinsically unstable under such high speed flow conditions.

2 Introduction

Supersonic combustion ramjet (scramjet) engines have exhibited great potential for the propulsion system of two-stage-to-orbit (TSTO) reusable launch vehicles, which can significantly lower the launching cost of payloads compared with rocket engines [1]. The development of reliable hypersonic air-breathing engines such as scramjets requires the appropriate solutions for many technical challenges, such as hypersonic and high temperature gas dynamics, fuel mixing and flame stabilization in supersonic flow, thermal protection, propulsion/vehicle integration, endothermic hydrocarbon fuel technology, the development of ground test facility, and the conduction of flight experiment. One of the most essential issues among these technical difficulties is the turbulent mixing and combustion of fuel in the combustors [2]. For a scramjet, the main flow throughout the combustor remains supersonic. Therefore, it only allows for a short residence time of fuel in a limited combustor length. The adequate mixing and combustion between fuel and air must finish in several milliseconds.

The LES method has achieved significant progress in modeling both non-reactive and reactive turbulent flows, and is considered to be a promising tool for large scale engineering applications [3]. The LES-LEM (linear eddy mixing) model [4] and the localized dynamic sub-grid closure [5] are used for compressible turbulent mixing and combustion in the German Aerospace Center (DLR) model combustor. The flamelet and PaSR sub-grid model are used for the LES of supersonic combustion in the Office National d'Etudes et de Recherches Aérospatiales (ONERA) [6], DLR [7,8] and the HyShot [9] model combustors under the framework of OpenFOAM [10]. Results are variously validated against the experimental measurements. Nevertheless, the interactions of the turbulence-chemistry, flame-shock, and shock-boundary layers, etc, remain to be great challenges. A better understanding of combustion characteristics in supersonic flows is desired for the large scale practical use of such air-breathing engines.

The objective of this paper is to study the highly compressible supersonic turbulent combustion process in a compact inlet/combustor model. The model is developed with the aim of investigating mixing, ignition, and combustion in supersonic flows at Stanford University [11]. Hydrogen is injected through a single wall flushed transverse injector. The PaSR sub-grid combustion model together with a skeletal mechanism of 9 species, 27 reaction steps hydrogen chemical kinetics are used in the LES solver. Results are analyzed on the structures of the flow and flame, the shock-shock and the flame-shock interactions.

3 The LES methodology

a. The governing equations and numerical schemes

The governing equations employed in this study are same as those presented in the previous work [8], and solved by the C++ library OpenFOAM combustion solver. The code employs a second order unstructured collocated finite volume method, in which the discretization is based on the Gauss theorem [7]. The time integration is stepped by the second-order explicit TVD Runge-Kutta scheme [12]. The maximum CFL numbers are no more than 0.3, resulting in physical time steps to be of the order of 10 ns.

b. The sub-grid combustion model and chemical kinetics

The mixed model is used for the sub-grid flow terms. The expression of the sub-grid stress tensor and flux vectors is given in [13]. The turbulence-chemistry closure is achieved by the PaSR sub-grid combustion model originally proposed in [14]. The detailed definition and the way how the chemical source terms are processed can be found there, which is not the task of the current work. This combustion model as well as its derivations have been proved to be effective in the modeling of supersonic turbulent combustion [7,8].

To investigate turbulent combustion using finite rate chemistry models, a reduced but still accurate kinetic mechanism is desired. The 9 reactive species (H_2 , O_2 , H_2O , H_2O_2 , HO_2 , O , H , N_2 , and OH), 27 reactions chemistry model in [15] is used, in which N_2 is regarded as inert species as its oxidation process has little effects on flame evolution in the combustor.

c. The computational configuration and boundary conditions

The inlet/combustor model is characterized by a compression inlet generating a shock train propagating into a constant area combustor section. It preserves the basic features of a practical scramjet, i.e. the inlet compression, the presence of shock waves generated by the inlet, the presence of confined space limited by the walls, and the complex interactions such as the flame-shock interaction, etc [11]. This configuration can be used for the early stage investigations on combustion zone structures and flame-shock interactions.

A two-dimensional schematic diagram of the computational model is shown in Fig. 1. The constant area section is 15 mm in height and 75 mm in width. The inlet entrance is 23 mm in height with a convergent

angle of 10° . The ramp inlet can generate a shock train that propagates along the combustor. The total length of the model is 315 mm. Hydrogen is injected through a single injector 70 mm downstream of the inlet at central of the combustor transversely into the air inflow, which flows under the nominally 8.0 Ma flight conditions. The fuel injector is designed to be under-expanded by a 2 mm diameter contoured nozzle. Details about the injector design can be found in [11].

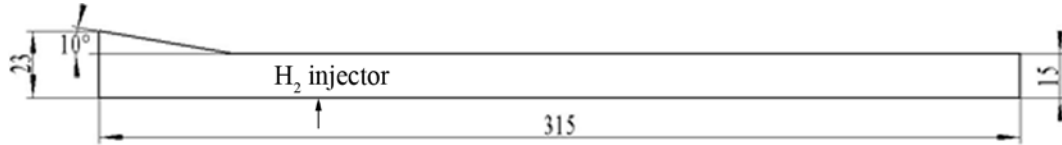


Figure 1. A schematic diagram of the computational model (All length dimensions are in *mm*)

Three different fuel injection conditions are studied in the original experiment work [11]. However, only the case with the lowest equivalence ratio is considered in the current paper. The fuel injection parameters and the inflow conditions at the model inlet under the nominal 8.0 Mach flight speed are listed in Table 1. The ground tests are carried out at the 6 Expansion Tube Facility of the High Temperature Gas Dynamics Laboratory at Stanford University [11]. However, it is not clear whether full combustion is achieved within the combustor in experiments. Therefore, the combustion efficiency will be calculated.

Table 1: The hydrogen injection parameters and the air inlet conditions

Type	p (kPa)	T (K)	Ma	U (m/s)	ER
Air inflow	40	1250	2.75	1900	0.08
Hydrogen jet	224.52	240	1.0	1180	

Three different types of boundary condition are used in the present study, i.e. supersonic inlet, supersonic outlet and slip walls. According to characteristic theory, all variables are prescribed at the inflow boundary as the flow under consideration is supersonic. Neumann conditions are used at outflow boundary in which all variables are extrapolated from interior while slip and adiabatic conditions are applied on all the walls. A refined mesh with more than 14.44 million hexahedral cells is adopted to resolve the detailed flow and combustion dynamics. Computation is continued until the second order statistical moments converge after more than ten flow-through times, of the order of 2.5 milliseconds.

4 Results and discussions

The LES solver and numerical approach have been validated in our previous works [8,16]. Therefore, the validation of numerical method is not presented here. In this section, the shock-shock and the flame-shock interactions around the fuel injector are studied. The combustion efficiency in this model is then calculated.

Figure 2 shows the temperature distribution near the upper wall (at the plane of $Y = 0.005$ m) as well as at seven uniform-spaced (0.03 m away from each other) cross-section planes. The X-planes are shifted away from their original locations in the combustor along Z direction to show them clearer. The first cross-plane ($X = 0.05$ m) locates shortly after the combustor entrance ($X \approx 0.0454$ m). The temperature shows very obvious regional characteristics. Generally, there are two different shock wave systems propagating in the combustor originated from two sources. The first shock system originates from the strong transverse fuel injector and is reflected mainly between the side walls and the central reacting shear layer. It is named as the injector-induced shock in this paper. The other shock system is generated by inlet and reflected mainly between the upper and lower walls. This is called the inlet-induced shock, which is much stronger than the

first one. It leads to the formation of intermittent large area of high temperature zone shown in the Y-plane. It is important to notice that both two wave systems are three-dimensional in space, and they also interact with each other and form complex wave structures in the combustor. However, the intersection of the injector-induced shock with the central reacting layer is too weak to be observed compared with the other two just mentioned.

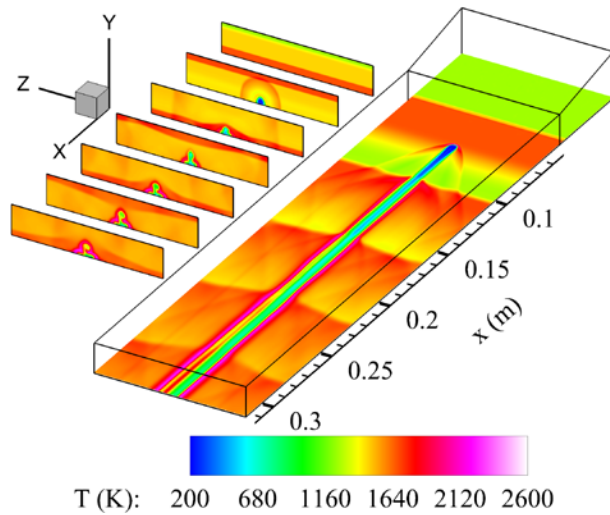


Figure 2. Temperature near the wall ($Y = 0.0005$ m)

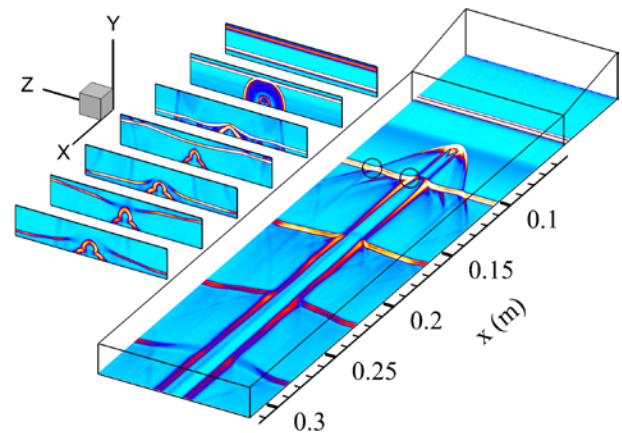


Figure 3. Numerical schlieren denoted by density gradient

Figure 3 shows the numerical schlieren image denoted by the magnitude of density gradient, $|\nabla \rho|$, to show the shock waves clearer. Both the two shock systems modify the flow field sharply, but the inlet-induced one shows stronger effect. However, due to the high stability of supersonic reacting shear layers [17], the both shocks are unable to propagate across the central reacting layers. It is of special interests to notice the two intersections of the injector-induced shock with the inlet-induced shock and the inlet-induced shock with the central reacting layer, which are all outlined by circles at the Y-plane in Fig. 3. Another important feature in Fig. 3 is the interaction between the inlet-induced shocks with the central reacting layers shown in the X-planes. The inlet-induced shocks locate alternatively at the lower and upper part of the shown X-planes, while the central reacting layers develop gradually along the X direction. When the inlet-induced shocks locate at the upper part of the X-planes (the second, fourth and sixth X-planes), they are too far to contact with each other. However, when the inlet-induced shocks locate at the lower part of the X-planes (the third, fifth and seventh X-planes), they are able to interact. With the development of reacting layers in the flow direction, they weaken the wall-reflected inlet-induced shocks and finally destroy their complete structures in the far enough downstream regions.

The shock-shock and shock-reacting shear layer interactions are discussed above. In practical combustion systems, however, another important phenomenon that exists is the flame-shock interaction. Here, only the interaction between the flame front around the fuel injector and the injector-induced shock is considered. Figure 4 shows the iso-surfaces of the second invariant of the velocity gradient tensor (Q), in which the $Y = 0.0005$ m plane shows the Mach number while the X-planes show the OH mass fraction. It can be seen that the transverse fuel injection induces strong bow shock and leads to vortex shedding which propagates shortly upstream of the injector. The iso-value of Q is chosen so that only the inlet-induced shock and its reflection on the upper and lower walls can be shown, but the reflection of the injector-induced shock on the side walls are too very to be apparently seen while the injector-induced shock itself is obvious enough. The OH radical is produced in reaction layers and consumed by slow recombination reactions. Therefore,

it is a marker of the hot products in high speed reacting flows [18]. From the X-planes shown in Fig. 4, it can be seen that the hot products develop slowly in the Y and Z planes along the X direction. Figure 5 shows pressure contours at different heights of the combustor, which indicate the three-dimension features and the development of shock wave systems in the combustor.

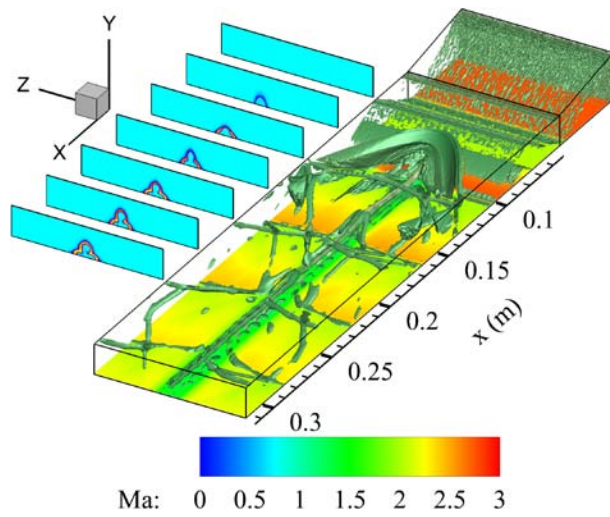


Figure 4. A schematic diagram of flame-shock interaction around the fuel injector, in which the Y-plane shows the Mach number and the X-planes show the OH mass fraction

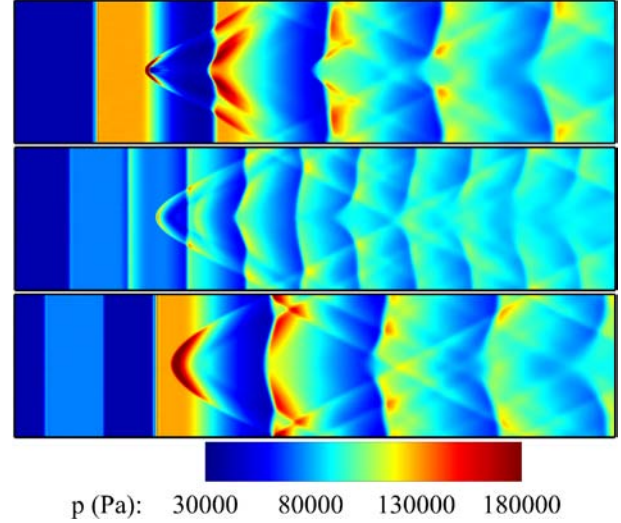


Figure 5. Pressure distribution at different combustor height (Y = 0.0005m, 0.0075 m, and 0.0145 m, respectively)

Combustion efficiency in this work is defined as the ratio of the actual H₂O formation to the ideal value, which can be expressed as [19],

$$\eta_c = \frac{m_{H_2O,real}}{m_{H_2O,ideal}} = \frac{\int_A Y_{H_2O} \rho u_x dA_{yz}}{\int_A Y_{H_2O} \rho u_x dA_{yz} + \frac{v_{H_2O} W_{H_2O}}{v_{H_2} W_{H_2}} \int_A Y_{H_2} \rho u_x dA_{yz}} \quad (1)$$

However, this definition does not take into consideration of the intermediate species, such as H, OH, HO₂, etc, which may also be converted to H₂O. Therefore, the ideal H₂O mass may be over-evaluated, leading to underestimated combustion efficiency. The combustion efficiency at the outlet is only around 36%.

5 Conclusions

A compact inlet/combustor model is numerically studied via large eddy simulation. Special attentions are paid on the shock-shock, flame-shock and shock-reacting layer interactions. The hydrogen-fueled model operates under nominal conditions of 8.0 M_{flight} . Basically, there are two shock wave systems propagating in the combustor originated from two different sources. The first one originates from the strong transverse fuel injector and is reflected mainly between the side walls and the central reacting shear layer, while the other one is generated by the inlet and reflected between the upper and lower walls. These two shock wave systems jointly control the very complex flow pattern under high inflow speed. The combustion efficiency is calculated at the outlet, which is quite low compared with cases of lower inflow speed.

References

- [1] Dissel AF, Kothari AP, Lewis MJ. (2005). Investigation of two-stage-to-orbit air-breathing launch vehicle configurations. AIAA paper 2005-3244.
- [2] Choi JY, Noh J, Byun JR, Lim JS, Togai K, Yang V. (2011). Numerical investigation of combustion/shock-train interactions in a dual-mode scramjet engine. AIAA paper 2011-2395.
- [3] Roux A, Gicquel LYM, Reichstadt S, Bertier N, Staffelbach G, Vuillot F, Poinso T. (2010). Analysis of unsteady reacting flows and impact of chemistry description in large eddy simulations of side-dump ramjet combustor. *Combust. Flame* 157: 176.
- [4] Génin F, Chernyavsky B, Menon S. (2003). Large eddy simulation of scramjet combustion using a subgrid mixing/combustion model. AIAA paper 2003-7035.
- [5] Génin F, Menon S. (2010). Simulation of turbulent mixing behind a strut injector in supersonic flow. *AIAA J.* 48: 526.
- [6] Berglund M, Fedina E, Fureby C, Tegnér J. (2010). Finite rate chemistry large-eddy simulation of self-ignition in a supersonic combustion ramjet. *AIAA J.* 48: 540.
- [7] Fureby C, Fedina E, Tegnér J. (2014). A computational study of supersonic combustion behind a wedge-shaped flameholder. *Shock Waves* 24: 41.
- [8] Huang ZW, He GQ, Qin F, Wei XG. (2015). Large eddy simulation of flame structure and combustion mode in a hydrogen fueled supersonic combustor. *Int. J. Hydrogen Energy* 40: 9815.
- [9] Fureby C, Chapuis M, Fedina E, Karl S. (2011). CFD analysis of the HyShot II scramjet combustor. *Proc. Combust. Inst.* 33: 2399.
- [10] OpenFOAM, OpenCFD Ltd. (2016). www.openfoam.com.
- [11] Gamba M, Miller VA, Mungal MG, Hanson RK. (2011). Ignition and flame structure in a compact inlet/combustor model. AIAA paper 2011-2366.
- [12] Gottlieb S, Shu CW. (1998). Total variation diminishing Runge-Kutta schemes. *Math. Comput.* 67: 73.
- [13] Bensow R, Fureby C. (2008). On the justification and extension of mixed models in LES. *J. Turbul.* 8: 1.
- [14] Chomiak J, Karlsson A. (1996). Flame liftoff in diesel sprays. *Int. Symp. Combust.* 26: 2557.
- [15] Marinov NM, Westbrook CK, Pitz WJ. (1995) Detailed and global chemical kinetics model for hydrogen. *Int. Symp. Transp. Proc.* 8: 1.
- [16] Cao DG, He GQ, Qin F, Wei XG, Liu B, Huang ZW. (2016). Investigation of shear layer growth influenced by shock waves in a scramjet. *AIAA J.* 54: 1133.
- [17] Barnes FW, Segal C. (2015). Cavity-based flameholding for chemically-reacting supersonic flows. *Prog. Aerosp. Sci.* 76: 24.
- [18] Micka DJ. (2010). Combustion stabilization, structure, and spreading in a laboratory dual-mode scramjet combustor. PhD thesis, The University of Michigan.
- [19] Liu G, Xu X, Xie YF. (2014). Numerical Investigation on the Supersonic Combustion of Liquid Kerosene in a Dual-Stage Strut Based Scramjet Combustor. AIAA paper 2014-3665.